Journal of Engineering and Applied Sciences 14 (Special Issue 8): 10251-10255, 2019
ISSN: 1816-949X

Improvement the Chemical Structure, Optical and Magnetic Properties of $CuFe_2O_4$ Thin Films

[1]Ghufran J. Abdulsada and [2]Zeina M. Kadam
[1]Department of Physics, College of Education,
[2]Department of Chemistry, College of Science, University of Al-Qadisiyah, Al Diwaniyah, Iraq

Abstract: In this research, the effect of Zn on the structural, optical and magnetic properties of the Ferrite-copper films $Cu_{1-x}Zn_xFe_2O_4$(CZF) precipitated on quartz glass substrate of x = 0, 0.5, 0.9 thickness of 450±10 nm and prepared by pyrolysis chemical spray method (400±10°C) and annealing (520°C) for 4h, through the X-ray diffraction spectrum. The crystalline structure of the prepared films was determined tetragonal spin ferrite in peak (211) and when it was doping with zinc, it turned into (cubic) in peak (311). The particle size found to decrease by increasing the concentration of Zn. The optical properties of the films were increased in the length of the energy gap before doping (2.74 eV) the energy gap increased by increasing doping to 2.88 eV when (x = 0.9). Typical values of magnetization and coercive force of the CZF films have been found to be Ms = 24.130 emu cm^{-3} and Hc = 260 Oe, respectively.

Key words: Magnetic material, ferrite, energy, coercive force, optical properties, spectrum

INTRODUCTION

The formula AB_2O_4 refers to spinal ferrites are very big class of oxides with a very large application in industry from simple permanent magnets to microwave application, magnetic recording, gas sensors (Pawar *et al*., 2011). The relative control of the magnetizations of the layers in these devices necessitates to pin the magnetization of the layers this is due to magnetically coupling this sheet to a hard one. To deposition thin films of ferrite (Jain *et al*., 2013), scientist have found a number of methods such as plating ferrite, sol-gel method, chemical method (Manikandan *et al*., 2013), electro deposition method, sputtering, RF sputtering and spin spray pyrolysis. Micro structure of thin film is an important parameter in determining their magnetic properties. Various growth parameters affect the micro structure of the films like substrate temperature during deposition (Brown and Forsyth, 1973) thermal expansion coefficient and lattice mismatch between the target and substrate. This research showed the morphological, optical (Caglar *et al*., 2006) structural magnetic properties of $Zn_xCu_{1-x}Fe_2O_4$ thin films prepared by spray payrolysis technique (Raghavender *et al*., 2015).

MATERIALS AND METHODS

Experimental section: $Zn_xCu_{1-x}Fe_2O_4$ thin films with [x = 0.0-0.9] were prepared by spray pyrolysis on substrate of SiO_2/Si at 400±10°C. Substrate cleaning plays an important role in the deposition of thin films because of the chemical deposition as the contaminated surface provided nucleation sites facilitating growth resulting into non-homogeneous film with different orientation and impurities $Zn_xCu_{1-x}Fe_2O_4$. Thin film were prepared by spray pyrolysis technique, analytic reagent grade chemical ($Fe(C_2O_4).2H_2O$), ($ZnCl_2$) ($Cu(NO_3)_2.3H_2O$) were used as raw materials, solutions were dissolved separately in de-ionized water at the concentration of 0.0 2 M for Zn^{+2} final solution were prepared by mixing these three solutions in 1:2 with the ratio of x = 0.0-0.9:

$$ZnCl_2 + 2H_2O \xrightarrow{heat} ZnO_{(s)} + Cl_{2(g)} + H_2O_{(L)} + H_{2(g)} \quad (1)$$

$$2Cu(NO_3)_2.3H_2O \xrightarrow{heat} 2CuO_{(s)} + 4NO_{2(g)} + O_{2(g)} + 3H_2O_{(L)} \quad (2)$$

$$Fe(C_2O_4) \xrightarrow{heat} FeO_{(S)} + CO_{2(g)} + CO_{(g)} \rightarrow 2Fe_2O_{(s)} + 1/2O_{2(g)} + heat \rightarrow \gamma\text{-}Fe_2O_3 \quad (3)$$

$$ZnO + (x)CuO + Fe_2O_{3(1-x)} \xrightarrow{heat} Zn_{(1-x)}Cu_xFe_2O_4 \quad (4)$$

RESULTS AND DISCUSSION

Structure properties: X-ray diffraction is used to reveal the structure of Cu-Zn Fe_2O_4 thin films prepared of a deposited and annealed. The structural analysis is essential for optimizing the properties needed for various applications. Figure 1 shows the XRD patterns of $CuFe_2O_4$. The data were analyzed using JCPDS standards card (No.08-0234) which confirms the spinal tetragonal structure. The diffraction patterns corresponding after annealing reveal that the film crystallize in polycrystalline preferred orientation along (211) plan type of tetragonal

Corresponding Author: Zeina M. Kadam, Department of Chemistry, College of Science, University of Al-Qadisiyah, Al Diwaniyah, Iraq

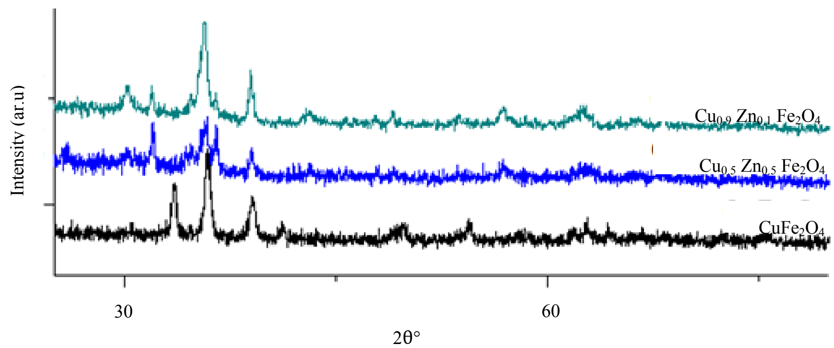

Fig. 1: X-ray diffraction patterns

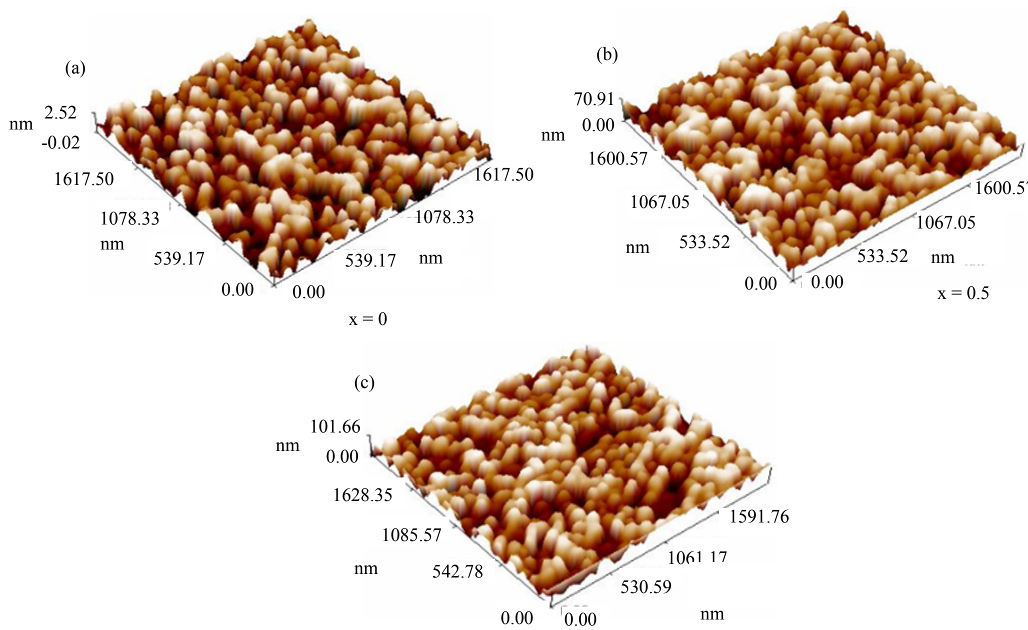

Fig. 2(a-c): Atomic force microscope images 3D for $Zn_xCu_{1-x}Fe_2O_4$ films (a) x = 0, (b) 0.5 and (c) x = 0.9

when (Zn^{+2}) was added to it turned into (a cubic) in peak (311). As Zn content increases then lattice parameter increases (x = 0.5, 0.9). Lattice constant of cu-Zn ferrite thin films which increases before doping to 8.363 Å because the radius of the ionic atom of the copper is smaller than the radius of the ionic atom of the zinc of the crystal and thus reduce average size. The lattice constant (a_o) calculated from equation:

$$a_o = d\sqrt{h^2+k^2+l^2}$$

The average crystallite size (D) was calculated by using Scherrer's formula:

$$D = (0.9\times\lambda)/(\beta\times\cos\theta)$$

Where:

λ : The wavelength of X-rays (1.5406)
β : The full-width at half-maximum in radian
θ : The angle of diffraction

It is seen that as the Zn content increases the crystallite size decreases from 17-11 nm (Table 1).

Atomic Force Microscopy (AFM): The topography of the surfaces of the prepared films and their impact on the same conditions were investigated at a temperature of 400±10°C. The high-power AFM was used to photograph and analyze these surfaces, at the measurement scale of 2×2 μm² values in Table 2. It was noted that the values of both the surface roughness and the square root of the average roughness is decreased by increasing the deflection ratio as well as decreasing average size by increasing the ratio of the deflection. This result is compatible with the results of the X-ray diffraction calculated of the rate of crystalline volume which was also increased by increasing the rate of deflection (Fig. 2).

Optical properties

Transmission (T): Figure 3 shows the relation between transmittance and wavelength in the range of 300-900 nm for copper-zinc ferrite thin films. The transmittance for all thin films increases as the wavelength increases in the wavelength range of about (400-700 nm) and then saturates at higher wavelengths .The spectrum shows high transmittance in the visible and infrared regions and low transmittance in the ultraviolet region.

Table 1: Lattice constant (a), crystallite size (D_{ave})

x-values	Lattice parameter (A°)	D (nm)
0.0	a = 5.8005, C = 8.5985	17.44
0.5	8.360	15.92
0.9	8.363	11.96

Table 2: Mean square root, surface roughness and particle size of films $Zn_xCu_{1-x}Fe_2O_4$) thin films.

Compound	Root mean square of roughness (nm)	Surface roughness (nm)	Grain size (nm)
$CuFe_2O_4$	0.727	0.629	91.22
$Zn_{0.5}Cu_{0.5}Fe_2O_4$	2.06	1.76	67.98
$Zn_{0.9}$ $Cu_{0.1}$ Fe_2O_4	18.1	15.4	88.94

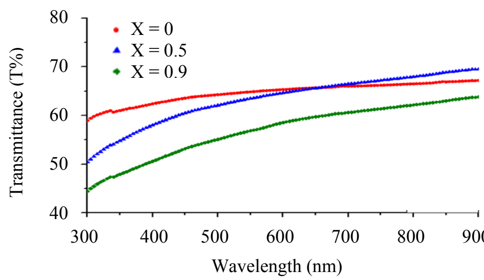

Fig. 3: Transmittance (T) versus wavelength (λ)

Absorbance (A): The variation of the absorbance spectrum with wavelength is opposite to the transmittance spectrum. The study of absorbance was in the range of 300-900 nm. Figure 4 shows the relation between absorbance (A) and wavelength for copper-zinc ferrite thin films. It is clear that absorbance decreases rapidly as the wavelength increases in the wavelength range of about (400-700) nm and then decreases slowly at higher wavelength.

It can be noticed that the absorbance decreases as the concentration of zinc increases and this can be attributed to the localized conductivity levels introduced by Zn^{2+} cations.

Energy gap (E_g): The optical energy gap was calculated for $Cu_{1-x}Zn_xFe_2O_4$ thin films with x = 0, 0.5, 0.9 by using the absorption coefficient values, Fig. 5 shows the plot of $(\alpha h\nu)^2$ vs. hν. The Energy gap (E_g) was determined by assuming the allowed direct transition between valance and conduction bands where, r = 1/2. The straight line is obtained which gives the value of the energy direct band gap. The extrapolation of the straight line to $(\alpha h\nu)^2 = 0$ gives value of the energy of direct band gap of the

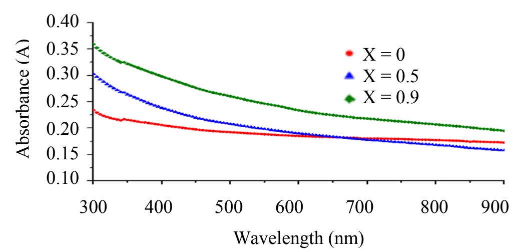

Fig. 4: Absorbance (A) versus wavelenght (λ)

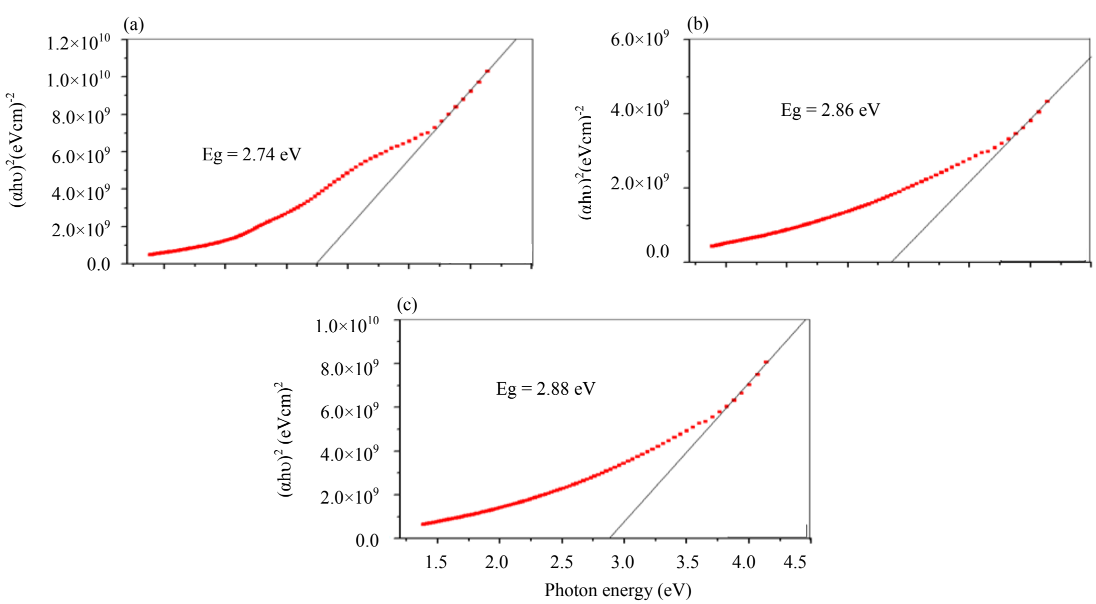

Fig. 5(a-c): The relation between $(\alpha h\upsilon)^2$ and (hυ) (a) x = (0.0), (b) x = 0.5 and (c) x = (0.9)

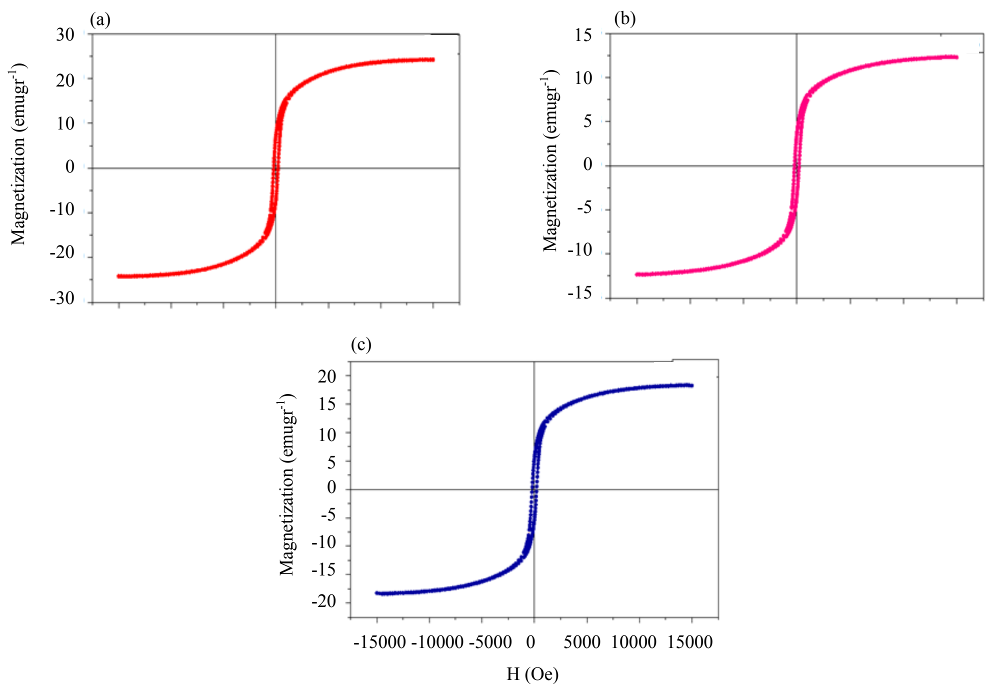

Fig. 6(a-c): The magnetic hysteresis ring of films ($Zn_xCu_{1-x}Fe_2O_4$) (a) x = 0, (b) x = 0.5 and (c) x = 0.9

material. The allowed direct band gap values range between (2.74 eV) for (x = 0.0) to (2.88eV) for (x = 0.9), Tauc's relation is used to calculate the optical band gap energy is given by in equation (Priyadharsini *et al*., 2009):

$$(\alpha\, hv) = B_x\, (hv\text{-}E_g)^r$$

where, α, E_g and hv are absorption coefficient, band gap energy and photon energy, respectively. About 'r' is equal to (2) for indirect and 1/2 for direct band-gap semiconductor, respectively (Deraz and Alarifi, 2012; Ravinder and Latha, 1999).

Magnetic properties (magnetic hysteresis): The results of the tests of magnetic retardation by Vibrating Sample Magnetometer (VSM), the magnetic hysteresis loop for Zn-CuFe_2O_4 ferrite are shown in Fig. 6. The saturation magnetization is found to decrease from 24.298-12.316 emg gm^{-1} with increase in Zn concentration from x = 0.0 to x = 0.5. The variation of saturation magnetization with ferrite composition can be explained on the basis of exchange interaction between irons at the tetrahedral (A) and octahedral (B).The replacement of Zn^{+2} ion by Cu^{+2} ion in the octahedral site would result in a decrease in saturation magnetization as the magnetic moment of Zn^{+2} ion is less than that of Cu^{+2} ion. The coercively values of the Zn-CuFe_2O_4 (x = 0.0, 0.5, 0.9) samples increases with zinc concentration due to the increase in the porosity with increasing dopant concentration. It is seen that the coercively is influenced by factors such as magneto-crystallinity, micro-strains, size distribution and domain size (Ravinder and Reddy, 2003; Dutta and Sinnha, 2011; Dutta *et al*., 2008) (Table 3).

Table 3: Saturation Magnetization (Ms), remanent Magnetization (Mr), coercivity (Hc)

X-values	M_s(emu gm^{-1})	M_r (emu gm^{-1})	H_c (Oe)
0.0	24.298	22.583	176.167
0.5	12.316	11.031	227.359
0.9	18.223	17.063	287.542

CONCLUSION

The results obtained from this study of the structural characteristics of $Zn_xCu_{1-x}Fe_2O_4$ films and in terms of (x = 0, 0.5, 0.9) showed that the process of attribution to the variable of the nature of crystalline structure. The prepared films are tetragonal type at the preferred direction (211) when doped with (Zn^{+2}) turned into a cubic type the preferred direction (311). Surface topography examined with AFM. It was observed that the deflection process resulted in a decrease in mean square root and surface roughness with decreasing average size distribution. From the optical properties was found that the increasing in transmittance and decrease in absorbance, the energy gap before doping (2.74 eV), the energy gap increased by increasing doping to 2.88 eV when (x = 0.9) showed an improvement in crystalline structure. The results of measurements of magnetic properties using VSM showed that all the prepared films were of soft ferrite type.

REFERENCES

Brown, P.J. and J.B. Forsyth, 1973. The Crystal Structure of Solids. Edward Arnold Publisher, London, UK., ISBN:9780844802053, Pages: 172.

Caglar, M., S. Ilcan and Y. Caglar, 2006. Influence of substrate temperature on structural and electrical properties of ZnO films. Trakya Univ. J. Sci., 7: 153-159.

Deraz, N.M. and A. Alarifi, 2012. Controlled synthesis, physicochemical and magnetic properties of nano-crystalline Mn ferrite system. Intl. J. Electrochem. Sci., 7: 5534-5543.

Dutta, A. and T.P. Sinha, 2011. Dielectric relaxation and conduction mechanism in $LaNi_{3/4}M_{1/4}O_3$ (M = Mo, W) at low temperature. J. Alloys Compd., 509: 1705-1710.

Dutta, A., C. Bharti and T.P. Sinha, 2008. Dielectric relaxation in Sr $(Mg_{1/3}Nb_{2/3})$ O_3. Phys. B. Condens. Matter, 403: 3389-3393.

Jain, A., R.K. Baranwal, A. Bharti, Z. Vakil and C.S. Prajapati, 2013. Study of Zn-Cu ferrite nanoparticles for LPG sensing. Sci. World J., 2013: 1-7.

Manikandan, A., J.J. Vijaya, L.J. Kennedy and M. Bououdina, 2013. Structural, optical and magnetic properties of Zn_{1-x} Cu_x Fe_2O_4 nanoparticles prepared by microwave combustion method. J. Mol. Struct., 1035: 332-340.

Pawar, D.K., S.M. Pawar, P.S. Patil and S.S. Kolekar, 2011. Synthesis of nanocrystalline Nickel-Zinc ferrite ($Ni_{0.8}$ $Zn_{0.2}$ Fe_2 O_4) thin films by chemical bath deposition method. J. Alloys Compd., 509: 3587-3591.

Priyadharsini, P., A. Pradeep, P.S. Rao and G. Chandrasekaran, 2009. Structural, spectroscopic and magnetic study of nanocrystalline Ni-Zn ferrites. Mater. Chem. Phys., 116: 207-213.

Raghavender, A.T., N.H. Hong, E. Chikoidze, Y. Dumont and M. Kurisu, 2015. Effect of Zinc doping on the structural and magnetic properties of Nickel ferrite thin films fabricated by pulsed laser deposition technique. J. Magn. Magn. Mater., 378: 358-361.

Ravinder, D. and K. Latha, 1999. Dielectric behaviour of mixed Mg-Zn ferrites at low frequencies. Mater. Lett., 41: 247-253.

Ravinder, D. and P.V.B. Reddy, 2003. High-frequency dielectric behaviour of Li-Mg ferrites. Mater. Lett., 57: 4344-4350.